PHYSICAL REVIEW A **81**, 043841 (2010)

CaF_2 ablation plumes as a source of CaF molecules for harmonic generation

M. Oujja,[1] R. de Nalda,[1] M. López-Arias,[1,2] R. Torres,[3] J. P. Marangos,[3] and M. Castillejo[1,*]

[1]*Instituto de Química Física Rocasolano, CSIC, Serrano 119, 28006 Madrid, Spain*

[2]*Unidad Asociada Departamento de Química Física I, Facultad de Ciencias Químicas, Universidad Complutense de Madrid, 28040 Madrid, Spain and Instituto de Estructura de la Materia, CSIC, Serrano 123, 28006 Madrid, Spain*

[3]*Blackett Laboratory, Imperial College London, SW7 2 BW London, United Kingdom*

(Received 23 December 2009; published 29 April 2010)

Generation of low-order harmonics (third and fifth) of the fundamental radiation of a *Q*-switched Nd:YAG laser (1064 nm, pulse 15 ns) was observed in a CaF_2 laser ablation plume. The ablation process is triggered by a second *Q*-switched Nd:YAG laser operating at 532 or 266 nm. In the scheme employed, the fundamental laser beam propagates parallel to the target surface at controllable distance and temporal delay, allowing to the probing of different regions of the freely expanding plume. The intensity of the harmonics is shown to decrease rapidly as the distance to the target is increased, and for each distance, an optimum time delay between the ablating laser pulse and the fundamental beam is found. *In situ* diagnosis of the plume by optical emission spectroscopy and laser-induced fluorescence serves to correlate the observed harmonic behavior with the temporally and spatially resolved composition and velocity of flight of species in the plume. It is concluded that harmonics are selectively generated by CaF species through a two-photon resonantly enhanced sum-mixing process exploiting the ($B\,^2\Sigma^+$–$X\,^2\Sigma^+$, $\Delta\nu = 0$) transition of the molecule in the region of 530 nm. In this work polar molecules have been shown to be the dominating species for harmonic generation in an ablation plume. Implications of these results for the generation of high harmonics in strongly polar molecules which can be aligned in the ablation plasma are discussed.

DOI: 10.1103/PhysRevA.81.043841 PACS number(s): 42.65.Ky, 52.38.Mf

I. INTRODUCTION

Laser-pulsed ablation of a solid target enables refractory species that are not usually found in the gas phase to be entrained in a gas flow. The atomic and molecular species (both neutral and ionized) that subsequently expand can then be used for a multitude of purposes, including media for harmonic generation (HG) and other nonlinear optical processes using intense pulsed lasers [1–3]. Solid target material so ablated offers a wide range of physical properties not readily available in gas phase samples (different ionization potentials, polarizabilities, intermediate resonances, and, in the case of molecules, differing geometries) that have the potential to extend the capabilities for generating coherent short-wavelength radiation. By optimizing plasma conditions through control of the laser ablation parameters (wavelength, energy, and duration of pulse, etc.) it is possible to enhance the efficiency and extend the harmonic cutoff. High-order HG in laser plasmas has been recently reviewed [3] and issues related with the selectivity of species in the plasma contributing to high harmonic generation (HHG), resonance-induced harmonic efficiency enhancement, and the effect on HG efficiency of large size particles such as clusters and nanoparticles have been discussed. These studies have mainly concentrated on targets constituted by metal, semiconductors, and fullerenes while dielectric materials have received much less attention [4–6]. Here we emphasize the possibilities of laser ablation plumes from dielectric materials as nonlinear optical media. Laser ablation of dielectrics is a source of molecular species of a wide range of dimensions [7–11], from diatomics to large polymeric chains, and therefore constitute good candidates to ascertain the role of molecular species in the HG in ablation plasmas.

In this work, we report studies performed in CaF_2, a highly ionic insulator with large band gap, widely used as material for optical windows and lenses. Laser ablation of this material has been the subject of numerous studies in order to determine laser damage thresholds and mechanisms [8–10]. Laser ablation plasma of CaF_2 yields Ca, F, and CaF as products [8–11], the latter being the most abundant. CaF is a molecule with a strong permanent electric-dipole moment (3.07 D for the ground state). This material provides an interesting case on the possibilities of using ionic dielectric solids as source of small molecular species with a high dipole moment amenable for HHG studies. The possibility of easy alignment and orientation of polar molecular species in a plasma plume, by applying an electric field in the region of interaction with the driving laser, opens the opportunity to more deeply understand the underlying physics of harmonic generation from molecular systems [12–15].

We report on the generation of low-order harmonics (third and fifth) of the fundamental radiation of a *Q*-switched Nd:YAG laser (1064 nm, pulse 15 ns) in a CaF_2 laser ablation plume. The ablation process is triggered by a second *Q*-switched Nd:YAG laser propagating orthogonally to the driving laser and operating at 532 or 266 nm. The harmonic signal is shown to depend on the probed spatiotemporal regions of the plasma while *in situ* spectroscopic analysis of spontaneous and induced plume emissions allows us to correlate the observed harmonic behavior with the composition and velocity of flight of species in the plume. The results shown extend the knowledge available on harmonic generation in ablation plasmas of refractory species and will help to address new issues on HHG on polar systems. Oriented polar molecules will support the generation of even harmonics (due

*Corresponding author: marta.castillejo@iqfr.csic.es.

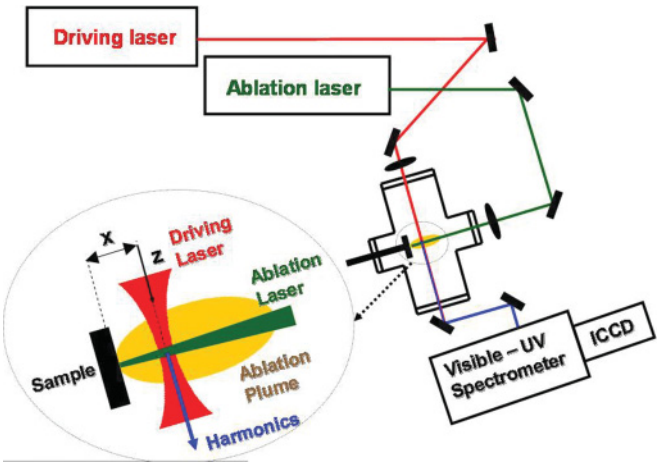

FIG. 1. (Color online) Experimental set up for harmonic generation in a CaF_2 ablation plume.

to the breaking of the center of symmetry); moreover, HHG mapping of the orbital of a polar molecule has not yet been studied and will prove an important test of current ideas of HHG-based molecular imaging.

II. EXPERIMENTAL

A CaF_2 ablation plasma was generated by focusing the second- or fourth-harmonic output (532 or 266 nm) of a Q-switched Nd:YAG (Quantel, Brilliant B, 6 ns FWHM) operating at a repetition rate of 10 Hz. This laser beam propagated perpendicularly to the surface of the target and was focused onto it by a 17-cm focal length lens to yield energy fluences up to 5 J/cm^2 (intensity 10^9 W/cm^2). The target, set on a rotating stage to avoid cratering of its surface, was placed in a vacuum chamber (background pressure 5×10^{-5} Pa). At a controlled delay, a 1064-nm driving pulse (Lotis TII LS-2147, 15 ns FWHM), propagating parallel to the target surface and at a distance between 0.6 and 2.1 mm, was focused on the ablation plume using a 25-cm focal length lens. Experiments were performed with driving laser intensities in the (1×10^9)–(6×10^9)-W/cm^2 range. A scheme of the experimental setup is shown in Fig. 1.

The plume emissions and the generated harmonics propagating collinearly with the driving laser were spectrally resolved with a resolution of 2 nm by a TMc300 Bentham monochromator equipped with a ruled grating (1200 lines/mm) coupled to an intensified charge-coupled-device (ICCD, 2151 Andor Technologies) operated in time-gated detection mode. The plume emissions from a 50-μm region across the propagation direction of the ablating laser were collected orthogonally using a $f = 8$ cm fused silica lens and imaged onto the entrance slit of the monochromator. The highly directional harmonics were also directed to the entrance slit of the monochromator by using a pair of dichroic mirrors. For measurements, the exposure time of the ICCD was set to 100 ns. Optically flat CaF_2, 5-mm-thick windows were used as targets. Each recorded measurement was taken on irradiation of a fresh (previously nonirradiated) region of the target.

III. RESULTS AND DISCUSSION

A. Plume emissions and harmonic generation

Spontaneous plume emission spectra were recorded with a constant gate width of 100 ns. Figure 2 shows the spectrum produced by irradiation of CaF_2 at 266 nm in a vacuum at 100 ns delay with respect to the arrival of the ablating pulse. The spectral lines can be readily assigned to neutral Ca and F atoms (Ca I and F I), singly charged ions (Ca II) [16], and bands of the green $B\,^2\Sigma^+$–$X\,^2\Sigma^+$ ($\Delta\nu = 0$) and orange $A\,^2\Pi$–$X\,^2\Sigma^+$ ($\Delta\nu = +1, 0, -1$) systems of the diatomic CaF [17] molecule. No continuous plasma emissions were detected under these conditions. The temporal evolution of the CaF_2 plume (Fig. 3) was monitored by measuring the intensity of emissions as a function of the delay between the arrival of the ablation pulse to the target and the opening of the acquisition temporal gate. It is observed that, for a given observation distance from the target surface, each emitting species reaches an intensity maximum at different times followed by a decay. At 0.6 mm from the target, emission from calcium ions (Ca II) reaches its maximum within the duration of the laser pulse while emissions from neutral species, F I and Ca I, attain maximum values at around 45 and 120 ns, respectively. Finally, the molecular CaF emission is temporally broader, with a plateau in the 400- to 600-ns interval. These results illustrate the different dynamics of generation, recombination, and flight velocities of species in the plume. The fast decay of ions is due to recombination with plasma electrons to yield neutral species. It is also observed that molecular species propagate at a velocity of flight (estimated in a region up to 2.1 mm from the target) of around 3×10^3 m/s, about 2–3 times slower than neutral atoms.

The thermodynamic parameters of the laser ablation plume, such as the plasma electron temperature (T_e) and number

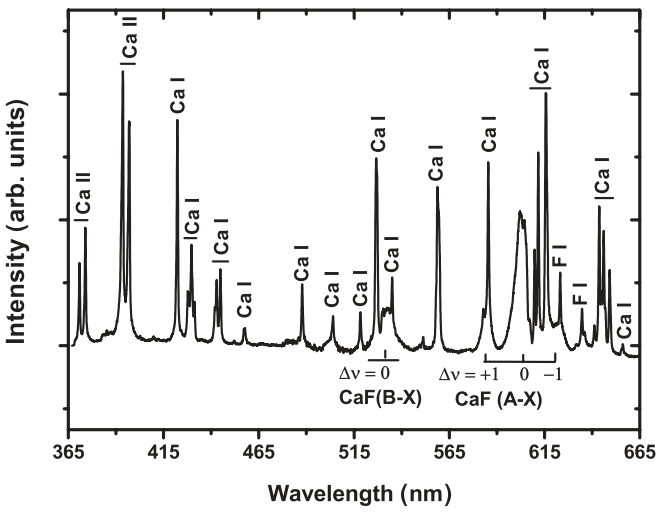

FIG. 2. Spontaneous emission spectrum upon ablation of a CaF_2 target at 266 nm and fluence of 5 J/cm^2 with assigned atomic and molecular emissions. Bands of Green $B\,^2\Sigma^+$–$X\,^2\Sigma^+$ ($\Delta\nu = 0$) and Orange systems $A\,^2\Pi^+$–$X\,^2\Sigma^+$ ($\Delta\nu = +1, 0, -1$) of the diatomic CaF molecule are indicated. The spectrum was acquired with a gate width of 100 ns at 100 ns delay with respect to the arrival of the ablating pulse by selecting a region of the plume at 0.6 mm from the target.

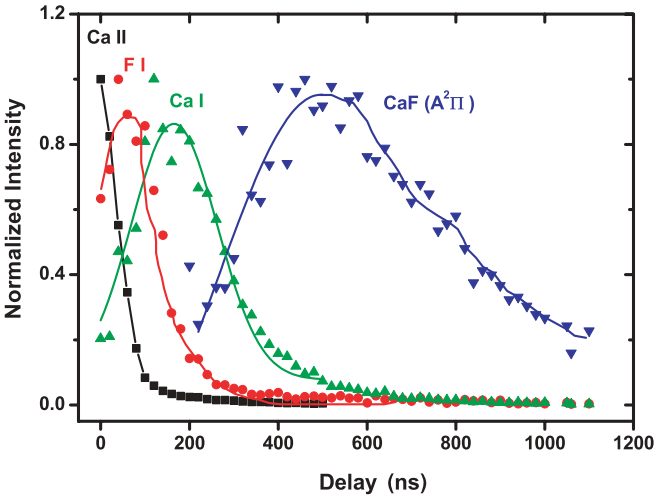

FIG. 3. (Color online) Evolution of normalized intensities of atomic and molecular emissions of a region 0.6 mm away from the target of the 266 nm CaF_2 plume, at a fluence of 5 J/cm^2, as a function of the delay between the ablation event and the aperture of the observation window. The gate width was set to 100 ns.

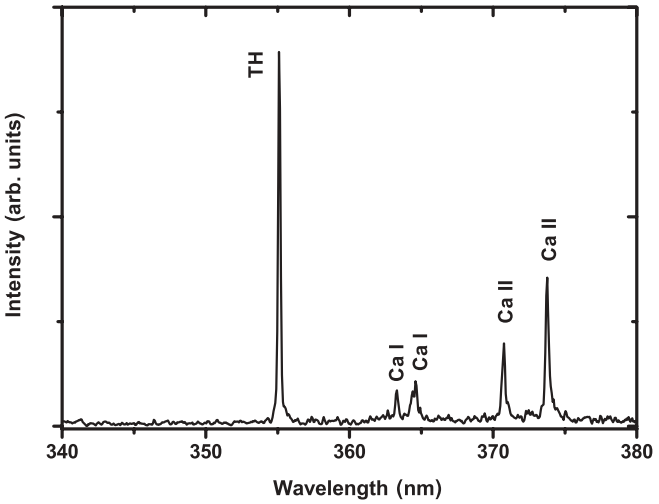

FIG. 4. Third harmonic of 1064 nm driving pulse generated in CaF_2 ablation plasma at a delay of 200 ns from the arrival of the ablating pulse of 266 nm (fluence of 5 J/cm^2). Assigned spontaneous Ca emissions are also marked.

density (N_e), were calculated assuming local thermodynamic equilibrium (LTE) [18] in the spatiotemporal regions of the plume explored (up to 2.1 mm from the target and up to 1 μs after ablation). Therefore, T_e values could be determined using the Boltzmann plot method [19] that relates the spectral intensity I_{mn} between two atomic energy levels m (upper) and n (lower) to T_e through the following equation:

$$\ln \frac{I_{mn}\lambda_{mn}}{A_{mn}g_m} = \ln \frac{N}{2} - \frac{E_m}{kT_e}, \qquad (1)$$

where λ_{mn} is the transition wavelength, A_{mn} the transition probability, and E_m and g_m the energy and statistical weight of the upper level, respectively. The temperature is obtained from the slope of the plot ln $[(I_{mn}\ \lambda_{mn})/(A_{mn}g_m)]$vs. E_m. Analysis was done using the atomic transitions listed in Table I which also displays the values of λ, A, g, and E [16]. With this method, we obtain a value of $T_e \approx 10^4$ K in the region of interest which is not sensitive to laser wavelength (532 or 266 nm).

The electron number densities N_e were determined by measuring the Stark broadening ($\Delta\lambda_s$) of one spectral line from the relation $N_e = \Delta\lambda_s \times 10^{16}/2\ W$, with W the electron impact parameter [20]. The contribution of other mechanisms of broadening can be neglected in the case of LTE, assumed in our ablation conditions. We measured the Stark broadening of the Ca I and Ca II lines indicated in Table I and used literature values of W [18]. For a value of $N_e \approx 10^4$ K (0.86 eV), the estimated N_e values are in the range of 10^{18}–10^{19} cm^{-3}.

Third and fifth harmonics (TH and FH) of the driving laser were observed as narrow line emissions at 355 and 213 nm, respectively. Figure 4 gives proof of the TH signature. An additional emission could be observed in the region of 530 nm when both ablation and fundamental beams were present. This emission, shown in Fig. 5, has been assigned to fluorescence induced by the driving laser (1064 nm) upon resonant two-photon absorption of diatomic CaF in its fundamental electronic state exploiting the $B\,^2\Sigma^+$–$X\,^2\Sigma^+$, ν'-ν'' = 5-5 and 6-6 vibrational transitions. The emission bands observed around 530 nm belong to the $\Delta\nu = 0$ vibrational sequence as indicated in Fig. 5. In order to confirm this assignment, the lifetime of this induced emission was measured by collecting the signal at increasing times with respect to the arrival of the driving pulse (inset of Fig. 5). The temporal decay can be fitted by an exponential function with a lifetime of 25 ± 1 ns, a value in good agreement with reported literature values for the CaF $B\,^2\Sigma^+$, $\nu = 0$ state [17].

TABLE I. Selected spectral lines and corresponding spectroscopic data [16] used for electron temperature calculations of CaF_2 laser induced plasma.

Plume species, λ (nm)	A_{mn} (10^7 s^{-1})	g_m	Transition	E_m (cm^{-1})
Ca I, 585 nm	6.60	5	$3p^64s^4p$–$3p^64\ p^2\ ^1P^o$–^1D	40719.487
Ca I, 610 nm	0.96	3	$3p^64s^4p$–$3p^64s^5s\ ^3P^o$–^3S	31539.495
Ca I, 611 nm	2.87	3	$3p^64s\ ^4p$–$3p^64s^5s\ ^3P^o$–^3S	31539.495
Ca I, 615 nm	4.77	3	$3p^63d^4\ s$–$3p^64s^5p\ ^3D$–$^3P^o$	31539.495
Ca II, 370 nm	8.80	2	$3p^64p$–$3p^65s\ ^2P^o$–^2S	52166.93
Ca II, 373 nm	17.0	2	$3p^64p$–$3p^65s\ ^2P^o$–^2S	52166.93
Ca II, 393 nm	14.7	4	$3p^64s$–$3p^64p\ ^2S$–$^2P^o$	25414.4
Ca II, 396 nm	14.0	2	$3p^64\ s$–$3p^64p\ ^2S$–$^2P^o$	25191.51

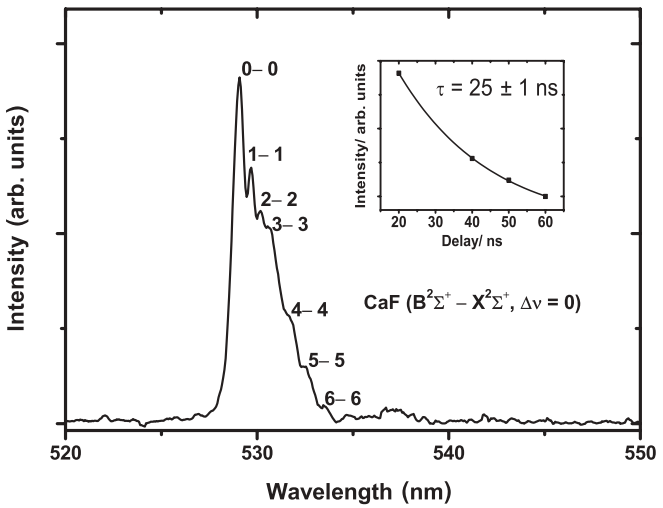

FIG. 5. Laser-induced fluorescence emission of the CaF (B-X, $\Delta v = 0$) system upon two-photon excitation by the fundamental driving laser at 1064 nm. The individual vibrational transitions are indicated. The delay between the ablation and driving pulses was set at 250 ns. The inset shows the temporal evolution of the induced emission measured by collecting the signal with a temporal gate of 20 ns at increasing times with respect to the arrival of the driving pulse.

Under the conditions of this experiment, the driving laser at 1064 nm serves as an *in situ* diagnostic probe of the CaF ($X\,^2\Sigma^+$) species owing to the fact that this wavelength meets a two-photon resonance condition in the diatomics. To extend the applicability of this tool for probing different molecular species in the plume of a wider range of dielectrics, a tunable driving laser or a third probe tunable laser would be required.

B. Characteristics of third and fifth harmonics

As mentioned in the previous sections, third and fifth harmonics of the driving laser were observed as narrow line emissions at 355 and 213 nm, respectively. It is important to obtain an estimate of the efficiency of this process. To this end, a strongly attenuated TH (or FH) of another Nd:YAG laser (355 or 213 nm) was made to propagate along the direction of propagation of the driving beam with similar propagation geometry and identical detection conditions to the TH emitted from the ablation plume. Attenuation was tuned so that the signal magnitude was comparable to that obtained from the TH generated in the plume. Measurement of the pulse energy prior to attenuation, together with a well-characterized attenuation factor, allowed us to estimate pulse energies, which provided an absolute reference for the energy of the TH emitted from the plume. Errors due to uncertainties in the divergence of the beams were minimized by using the widest slits possible in the monochromator and checking that no significant spatial selection was taking place. This procedure yielded an efficiency value of $\approx 4 \times 10^{-5}$ for the TH and 10^{-5} for the FH.

It is likely that higher odd harmonics would be generated as well in the present experimental conditions, but their efficiency should be considerably lower, and their observation would require a setup with vacuum ultraviolet range capabilities.

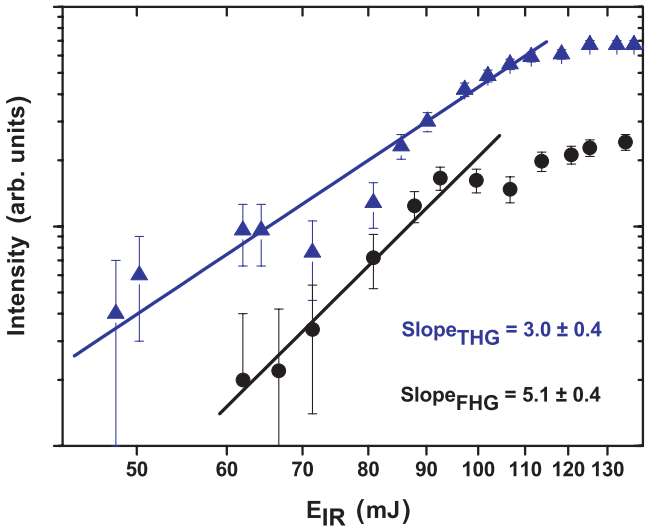

FIG. 6. (Color online) Behaviour of the third and fifth harmonic generated in a 532 nm CaF_2 ablation plume as a function of the fundamental laser intensity (at 1064 nm). Both signals show the expected power laws for low intensities, followed by a saturation region above 100 mJ (corresponding to an intensity of 2×10^9 W/cm^2).

Both observed harmonics display the expected power laws for low intensities (Fig. 6), followed by a saturation region above 100 mJ (corresponding to an intensity of 2×10^9 W/cm^2 intensity). The intensity of the third and fifth harmonic signals varies as the IR fundamental laser focus position is scanned across the ablation plume in the laser propagation direction (z scan). Figure 7 shows results obtained by ablating the target at 266 nm. The experimental points were fitted by Gaussian functions of the form $y = A \exp(-2x^2/w^2)$ yielding widths of $w = 20 \pm 1$ and 9.0 ± 0.5 mm for the third and fifth harmonics, respectively. A considerably broader structure is found for the

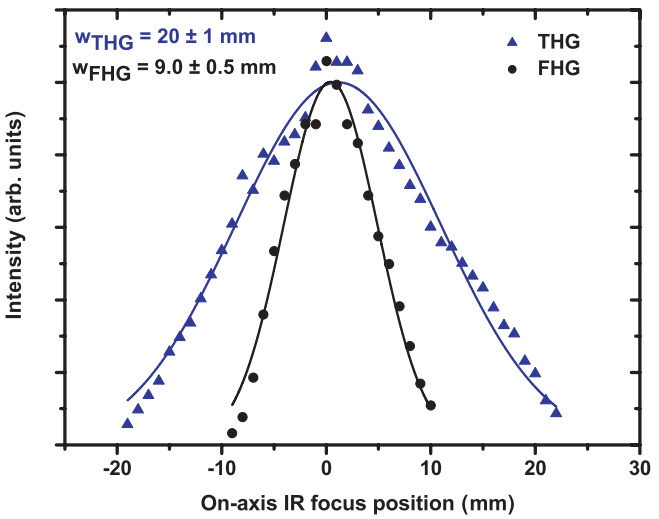

FIG. 7. (Color online) Intensity of third and fifth harmonic signals as the 1064 nm driving laser focus position is scanned in the propagation direction (z scan) across the 266 nm laser-induced ablation plume, maintaining the distance (1 mm) to the surface of the CaF_2 target. Experimental points are shown together with Gaussian fits with the widths indicated on the graph.

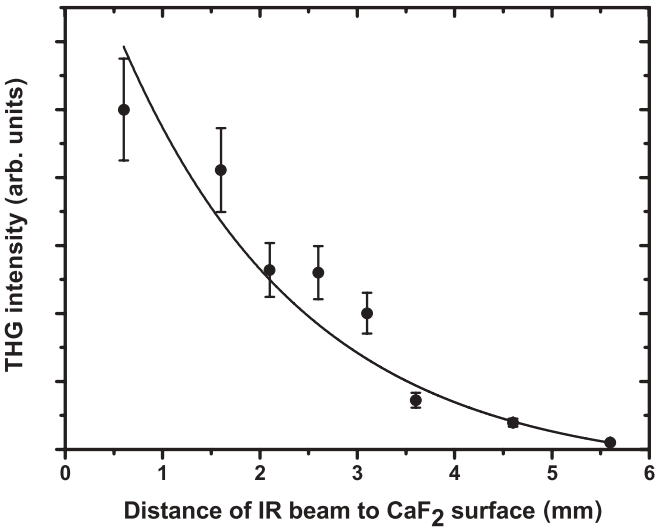

FIG. 8. Intensity of third harmonic signal at 355 nm as the position of the fundamental IR beam is displaced from the surface of the CaF_2 target (x axis in Fig. 1). For each distance probed, the delay between the ablation beam at 266 nm and the fundamental beam was set at the value corresponding to the optimum signal.

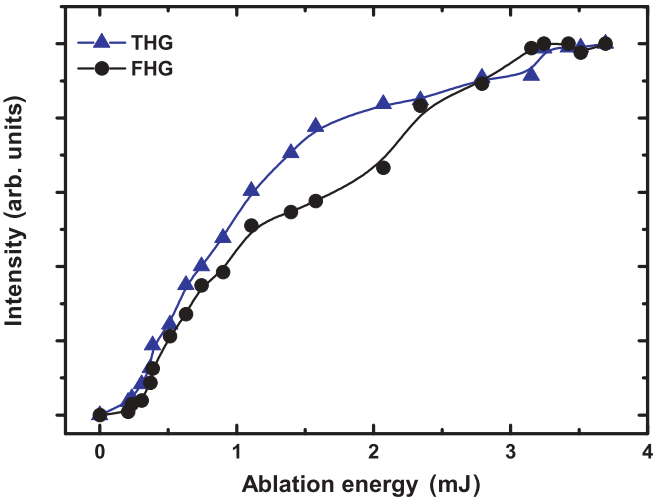

FIG. 9. (Color online) Dependence of third and fifth harmonics generated in CaF_2 ablation plume with the 266 nm ablation laser pulse energy (the maximum energy corresponds to a fluence of 5 J/cm^2). The fundamental IR intensity was fixed at 6×10^9 W/cm^2, the target-IR beam distance was 1 mm and the ablation-probing delay was 250 ns. The lines are simply guides to the eye.

TH beam as expected, given the sharper intensity dependence of the FH signal and the density profile of the ablation plume.

As mentioned previously, the intensity of harmonics signals changed dramatically with the distance of the fundamental IR beam to the surface of the CaF_2 target. A representative result is given in Fig. 8, obtained on ablation of the target at 266 nm. It is observed that the harmonic signal is no longer visible for distances higher than 5 mm away from the target.

The expected quadratic behavior of harmonic emission intensities as a function of local density of the nonlinear medium [21] can also be indirectly measured through their dependence on ablating laser fluence, since higher fluences correspond to higher material quantities ejected from the CaF_2 target and, thus, to higher densities. This measurement is displayed in Fig. 9.

As described in the previous section, the ablation plasma is composed of atomic and molecular species, both in fundamental and electronically excited states, and clusters or nanoparticles; these can contribute in various extents to the harmonic generation process. Investigations of TH generation in pure Ca vapors [22] have reported resonance enhancement of the yield by exploiting autoionizing states of the metal. These processes serve to generate radiation at fixed and tunable wavelengths in the vacuum ultraviolet range, a different spectral region that the one covered by the present study. The mixture of species has traditionally been considered a strong disadvantage of ablation plumes as compared with atomic or molecular jets for the generation of harmonics. However, in this case we have been able to unambiguously identify the main species acting as nonlinear medium, mainly through the study of the temporal evolution of the harmonic signal. Figure 10 compares the temporal evolution of the third and fifth harmonic signals with the laser-induced fluorescence of the CaF B-X system, both as a function of time delay between the ablation event in CaF_2 and the arrival of the fundamental IR laser near the surface of the sample. It is clear that the three observables follow an almost identical temporal pattern, with the FH showing slight deviations that can be attributed to minor experiment-to-experiment variations in the expansion conditions. Therefore, although some contribution to harmonic generation from atomic and electronically excited molecular species in the plume could not be totally excluded (see Fig. 3), it is believed that the CaF molecule in its ground electronic state, produced in the plasma with much higher number densities than its atomic counterparts [8], is the main source of harmonic generation. The general value of this finding should

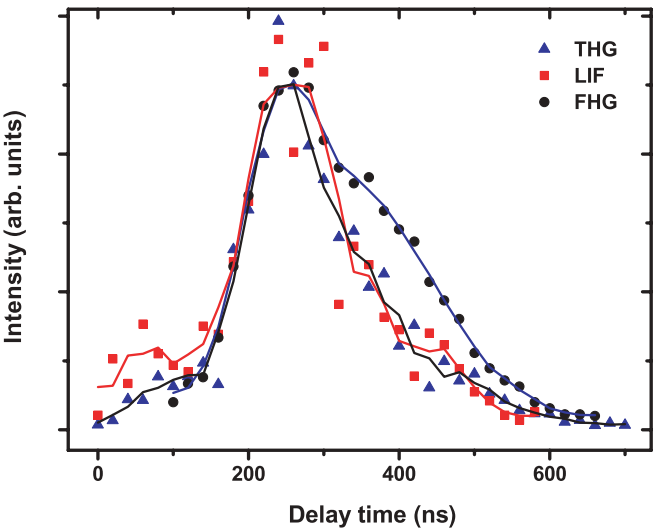

FIG. 10. (Color online) Temporal evolution of third harmonic generation (THG), fifth harmonic generation (FHG) and laser-induced fluorescence of the CaF B-X system (LIF) as a function of time delay between the ablation event in CaF_2 (initiated by 5 J/cm^2 at 266 nm) and the arrival of the fundamental IR laser (1064 nm) at 1 mm from the surface of the sample.

not be overlooked. In fact, preliminary studies in a wide range of ionic solids, such as MgF_2, NaCl, etc., indicate that the formation of strongly polar diatomic molecules (MgF, NaCl, etc.) in the plume is favourable, and therefore dominance of these strongly polar species as source for HG is foreseen in the ablation plumes of these materials.

On the other hand, in the case of CaF, the B-X, $\Delta v = 0$ transition is in resonance with a two-photon absorption of the driving laser in the CaF molecule, a condition that contributes to the enhancement of the nonlinear susceptibility for the harmonic generation process and henceforth to the harmonic yield. More work is in progress to ascertain the role of this resonance on the efficiency of the process by scanning a tunable driving source across the two-photon resonance. The use of a tunable source, as mentioned above, will also constitute a tool for ascertain the role of small size molecular species in the HG process induced in plumes of other materials. In the present case, the photon energies of the third and fifth harmonics of the driving frequency are below the ionization potential of the CaF molecule (5.84 eV) [23]. Therefore no enhancement of the generation yield is expected from molecular resonances within the ionization continuum and self-absorption by the molecular ionization continuum should not contribute to its reduction.

Apart from its dependence on the driving laser power, density of species, and susceptibility, the harmonic generation yield is dependent on the phase shift $b\Delta k$, where b is the confocal parameter, through the phase optimization integral $F(b\Delta k)$ [21]. In the experimental conditions herein, $b \gg L$ (plane-wave approximation), with L the length of the nonlinear medium which is assumed to be equal to the plume dimension in the direction perpendicular to the ablation laser (around 20 mm, see Fig. 6). The total phase mismatch between the generated harmonic and the driving polarization includes a geometrical factor, equal to $2(q-1)/b$ for a Gaussian beam, a dispersive term, and a contribution from coexisting free electrons in the plasma [2], the latter being of the order of 10^{-9}–10^{-8} cm^{-1}. Since the coherence length associated with all these sources of phase mismatch is considerably larger than the plume dimensions, it is possible to assume that the harmonic generation process is practically phase matched.

Of special interest is the extension of the work reported here to generation of shorter wavelength radiation, i.e., higher-order harmonics, driven by short laser pulses in the femtosecond range. Enhancement of high-order nonlinear processes through exploitation of intermediate resonances is expected within perturbation theory and has been studied theoretically by Gaarde and Schafer [24]. For nanoparticle-containing plumes, the phenomenon has recently been reported by Ganeev *et al.* [25], where a two-photon surface-plasmon resonance with the driving laser produced a considerable enhancement in all harmonic orders detected. In the strong field regime characteristic of HHG processes, it is expected that the AC Stark effect plays an important role and can drive nearby transitions into resonance [26]. This work shows that CaF is an ideal candidate for HG studies in polar species but also suggests that ablation of ionic dielectrics is a source of gas phase small polar molecules that can be used for HHG. Additionally, the large oscillator strength of the B-X transition in CaF and similar diatomics constitutes an excellent test case for the study of the role of resonances in these highly nonlinear processes.

IV. CONCLUSIONS

Third and fifth harmonics of a driving 1064-nm, 15-ns pulse are generated in a CaF_2 ablation plume triggered by 6-ns laser pulses of 532 or 266 nm. Harmonics are selectively generated by the CaF species through a two-photon resonantly enhanced sum-mixing process exploiting the (B-X, $\Delta v = 0$) transition of the molecule around 530 nm. Ablation conditions ensure a negligible degree of phase mismatch. The strong evidence for CaF being the dominant species for THG and FHG in these measurements suggests extension to a wider range of ionic dielectrics able to yield strongly polar diatomics and to higher-order nonlinear optical processes. In particular, HHG from CaF, and similar strongly polar, molecules in the plume and the application of an additional laser pulse for its alignment is a realistic possibility. Other polar molecules can be entrained in the gas phase by ablation (MgF, NaCl, etc.). In that case modulation of the HHG signal at an alignment revival of the molecule would be a strong signature of the HHG from that species, permitting detailed quantitative studies of HHG from an aligned (and potentially oriented) ensemble of polar molecules.

ACKNOWLEDGMENTS

Funding from MEC, Spain, Project CTQ2007-60177 is gratefully acknowledged. We thank support of EU ITN FASTQUAST. M.O. thanks CONSOLIDER CSD2007-00058 for support.

[1] S. Kubodera, Y. Nagata, Y. Akiyama, K. Midorikawa, M. Obara, H. Tashiro, and K. Toyoda, Phys. Rev. A **48**, 4576 (1993).
[2] W. Theobald, C. Wülker, F. P. Schäfer, and B. N. Chichkov, Opt. Commun. **120**, 177 (1995).
[3] R. A. Ganeev, J. Phys. B: At. Mol. Opt. Phys. **40**, R213 (2007).
[4] R. A. Ganeev, M. Suzuki, M. Baba, M. Ichihara, and H. Kuroda, J. Opt. Soc. Am. B **25**, 325 (2008).
[5] R. A. Ganeev and D. B. Milošević, J. Opt. Soc. Am. B **25**, 1127 (2008).
[6] R. A. Ganeev, H. Singhal, P. A. Naik, I. A. Kulagin, P. V. Redkin, J. A. Chakera, M. Tayyab, R. A. Khan, and P. D. Gupta, Phys. Rev. A **80**, 033845 (2009).
[7] E. Rebollar, M. Oujja, G. Bounos, A. Kolloch, S. Georgiou, and M. Castillejo, J. Appl. Phys. **101**, 033106 (2007).
[8] R. C. Estler, E. C. Apel, and N. S. Nogar, J. Opt. Soc. Am. B **4**, 281 (1987).
[9] R. Mitzner, A. Rosenfeld, and R. König, Appl. Surf. Sci. **69**, 180 (1993).

[10] S. Gogoll, E. Stenzel, H. Johansen, M. Reichling, and E. Matthias, Nucl. Instrum. Methods Phys. Res. B **116**, 279 (1996).
[11] B. S. Zhao, M. Castillejo, D. S. Chung, B. Friedrich, and D. Herschbach, Rev. Sci. Instrum. **75**, 146 (2004).
[12] R. Velotta, N. Hay, M. B. Mason, M. Castillejo, and J. P. Marangos, Phys. Rev. Lett. **87**, 183901 (2001).
[13] E. Lorin, S. Chelkowski, and A. D. Bandrauk, New J. Phys. **10**, 025033 (2008).
[14] Y. Mairesse, J. Levesque, N. Dudovich, P. B. Corkum, and D. M. Villeneuve, J. Mod. Opt. **55**, 2591 (2008).
[15] L. Holmegaard, J. H. Nielsen, I. Nevo, H. Stapelfeldt, F. Filsinger, J. Küpper, and G. Meijer, Phys. Rev. Lett. **102**, 023001 (2009).
[16] NIST Atomic Spectra Database, http://physics.nist.gov/PhysRefData/ASD/index.html.
[17] L. E. Berg, K. Ekvall, and S. Kelly, Chem. Phys. Lett. **257**, 351 (1996).
[18] H. R. Griem, *Plasma Spectroscopy* (McGraw-Hill, New York, 1964).
[19] *Plasma Diagnostic Techniques*, edited by R. H. Huddlestone and S. L. Leonard (Academic Press, New York and London, 1965).
[20] *Principles of Laser Plasmas*, edited by G. Bekefi (Wiley, New York, 1976).
[21] J. F. Reintjes, *Nonlinear Optical Parametric Processes in Liquids and Gases* (Academic Press, Orlando, 1984).
[22] W. Jamroz and B. P. Stoicheff, in *Progress in Optics*, edited by E. Wolf, Vol. 20 (North-Holland, Amsterdam, 1983), pp. 326–380.
[23] J. E. Murphy, J. M. Berg, A. J. Merer, Nicole A. Harris, and R. W. Field, Phys. Rev. Lett. **65**, 1861 (1990).
[24] M. B. Gaarde and K. J. Schafer, Phys. Rev. A **64**, 013820 (2001).
[25] R. A. Ganeev, M. Suzuki, M. Baba, M. Ichihara, and H. Kuroda, J. Phys. B: At. Mol. Opt. Phys. **41**, 045603 (2008).
[26] R. A. Ganeev, M. Suzuki, M. Baba, H. Kuroda, and T. Ozaki, Opt. Lett. **31**, 1699 (2006).